Numerical Study on Blade Roughness Effect
on the performance of turbomachines

Shin-Hyoung Kang[1] and Young-Seok Kang and Kyung-Ho Han[2]

[1] Department of Mechanical Engineering
Seoul National University
San 56-1, Sin-lim dong, Gwan-Ak Gu, Seoul 138-226, KOREA
Phone: +82-2-880-7113, FAX: +82-2-883-0179, E-mail: kangsh@snu.ac.kr
[2]School of Mechanical Engineering Seoul National University

ABSTRACT

Blade roughness effects on performances and flows of axial compressor and axial turbine stages are numerically investigated. A wall function option for roughened wall boundary condition is available in TascFlow code. Flow calculations on the flat plate with various roughness show that normalized wall velocity drop due to roughness is coincidence with that of Prandtl-Schlichting's empirical relation. Flow calculations through an multi-stage compressor and turbine stage showed that roughness increases boundary layer thickness which increases pressure loss and reduces their efficiencies. Work transfer from rotor to blade in the compressor decreases, however work transfer in the turbine increases gradually as roughness height increases.

One-dimensional analysis is done to estimate these differences quantitatively with absolute flow angle change and additional loss generation due to roughness. The efficiency drop is dominated by pressure loss due to roughness.

INTRODUCTION

Blade surface of turbomachines could experience significant degradation in shape or roughness due to harsh operating environment. In most cases it is known that blade surface becomes rough due to deposition, erosion or pitting. Sometimes blade roughness suppresses flow separation and shows positive effect on the performance. However, roughness usually increases blockage due to the thickened boundary layer on the passage surface, which results in the performance and efficiency decreases. Operation of best performance and efficiency becomes an important issue now considering total cost of operation and maintenance during a life cycle of machinery. Therefore understanding the effects of blade roughness on the flow and performance is important aspects not only in design but also in operation and maintenance.

If blades or walls become rough for any reason, even a small roughness will break up the thin viscous inner layer and greatly increase the wall friction and heat transfer coefficient. As a result total pressure loss can be increased. Blade roughness effect therefore is considered to be one of the main sources of pressure loss. For this reason, many previous researchers tried to clarify the relationship between loss increase and blade or wall roughness.

Main concerns of early days' researchers were that it could be possible for many kinds of roughness elements such as uniform sand, sand mixtures, rivets, threads, spheres, etc. can be expressed in one length scale. Also they tried to obtain correlations between average roughness height and representative roughness height. Speidel and Nikuradse(1954) defined equivalent sand-grain roughness k_s, which is the function of roughness Reynolds number and friction coefficient.

$$k^+ = \text{Re}(k_s / c)\sqrt{C_f / 2} \qquad (1)$$

Prandtl and Schlichting defined the three roughness regimes.

$$k^+ < 4 \qquad : \text{hydraulically smooth wall}$$
$$4 < k^+ < 60 \quad : \text{transitional-roughness regime}$$
$$k^+ > 60 \qquad : \text{fully rough flow}$$

Forster(1967) showed that normalized sand-grain roughness of $k_s / l = 2.8 \times 10^{-3}$ in turbine caused 6% decrease in efficiency. Another study was reported by Bammert and Sandstede(1972) that roughness $k_s / l = 10^{-3}$ to 10^{-2} decreased efficiency from 5 to 10% compared to smooth surfaces. Apart from focusing on sand-grain, another trend of roughness study is clarifying the mechanism of loss generation by examining flow field closely. Bammert and Sandstede showed that blade roughness caused rapid boundary layer transition and increase of friction coefficient by experiment with low speed turbine cascade. Kind et al.(1998) reported that in cascade experiment, suction side surface is more sensitive to pressure side surface in deposition or erosion. So far, despite a number of experimental researches have been reported, few CFD researches have been announced concerned with roughness effect on the performance or flow field. If CFD results are reliable in predicting the performance or flow field with roughness effect, it is possible to describe the loss generation mechanism associated with flow field more detailed. Also dependency on the experimental results to build database for many cases will be reduced.

In this paper, CFD method was tried to predict roughness effect on the flow field and the overall performance of compressor and turbine stages. Commercial CFD code, TascFlow is used to predict flow field with roughness model. At first, to validate roughness model in TascFlow, CFD calculation of flat Plate with different sand-grain roughness height and Reynolds number is carried out. After that, third stage of Low Speed Research Compressor and first stage of commercial gas turbine are computationally simulated to investigate the effect of blade roughness on the performance and flow field.

NOMENCLATURE

C_f	: Friction coefficient
C_p	: Pressure coefficient
P'	: Normalized pressure
R	: Normalized radius

T	: Temperature, Torque
c	: Speed
h	: Enthalpy
k	: Average roughness height
k_s	: Sand-grain roughness height
k^+	: Roughness Reynolds number
p	: Pressure
r	: Radius
u_t	: Rotor tip speed
u^+	: Normalized wall velocity
Δu^+	: Offset of wall-velocity
y^+	: Normalized wall distance
$\dot{m}$	: Mass flow rate
α	: Absolute flow angle
β	: Relative flow angle
ϕ	: Flow coefficient
η	: Efficiency
ρ	: Density
ω	: Angular velocity
ξ	: Loss coefficient
ψ	: Head coefficient or Work coefficient

ROUGHNESS MODEL VALIDATION.

Developments of turbulent boundary layer in a flat plate are calculated to validate roughness model in the Tascflow. Fig. 1 shows schematic diagram of flat plates. The flat plate has no thickness and is 10m long. CFD grid consists of two flat plates and flow region between two plates. Space between two plates is sufficiently far to avoid boundary layer interactions. Computational simulation is carried out for 5 different sand-grain roughness heights, smooth wall and k_s = 0.1, 0.2, 0.5, 1mm respectively. Inlet speed is set to10, 100m/s. By changing inlet speed and sand-grain roughness height, roughness Reynolds number k^+ can be changed and roughness model in TascFlow can be validated for wide range of k^+. The range of k^+ is 20~300 and corresponding range of Reynolds number is 10^5~10^8. Exit pressure is 1atm and k-ω high Reynolds turbulence model is used with free stream turbulence intensity of 3%.

Although wall roughness affects near wall velocity profile, the logarithmic layer still exists. As k^+ increases the intercept begins to move downward monotonically with the quantity of Δu^+ in Eq. (2).

$$u^+ = \frac{1}{0.41}\ln y^+ + 5.0 - \Delta u^+ \qquad (2)$$

The value of Δu^+ is usually a function of the roughness type, and height. But as mentioned before every type of roughness can be expressed in equivalent sand-grain roughness height and Prandtl and Schlichting(1956) proposed a correlation based on many
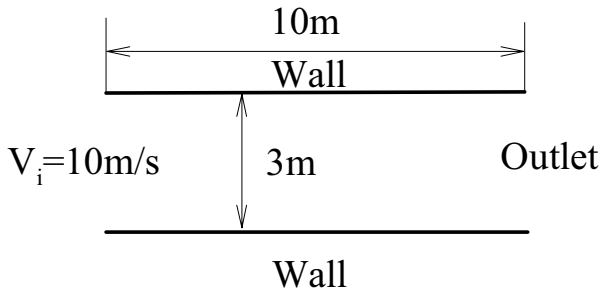
Fig. 1 schematic diagram of flat wall for validation

empirical results for sand-grain roughness that is called classic Prandtl-Schlichting sand-grain roughness curve.

On the other hand, Tascflow employs Eq.(3) to predict wall-velocity when roughness appear. It is a linear fitting equation based on many empirical results for sand-grain roughness.

$$\Delta u^+ = \frac{1}{0.41}\ln(1+0.3k^+) \qquad (3)$$

In CFD code, accurate roughness model should predict quantity of Δu^+ in reasonable value that in this study, CFD results are compared with Prandtl-Schlichting's roughness curve in Fig. 2. When k^+ <10, in smooth regime, difference between Prandtl-Shclichting's roughness curve and Eq.(3) and CFD results becomes large. But in most transitional-roughness regime and fully rough regime, which is the operating range of turbomachines, two equations and CFD results are well agreed. Maximum difference between CFD results and Prandtl-Shclichting's curve is about 10%.

Also friction coefficient C_f at wall is compared to empirical correlations. Eq. (4) represents friction coefficient for smooth wall, and Eq. (5) and Eq. (6) for Transitional-roughness regime and fully rough regime respectively.

$$C_f \approx \frac{0.027}{\mathrm{Re}_x^{1/7}} \qquad (4)$$

$$\mathrm{Re}_x \approx 1.73(1+0.3k^+)e^z\left(z-4z+6-\frac{0.3k^+}{1+0.3k^+}(z-1)\right) \quad (5)$$

(where $z = 0.41(2/C_f)^{1/2}$)

$$C_f \approx \left(2.87+1.58\log\frac{x}{k}\right)^{-2.5} \qquad (6)$$

Fig. 3 shows that friction coefficients of CFD with wall Friction coefficients calculated from CFD results are well agreed with those of fitting equations in high Reynolds number region. But in low Reynolds number region CFD and correlations are not well agreed
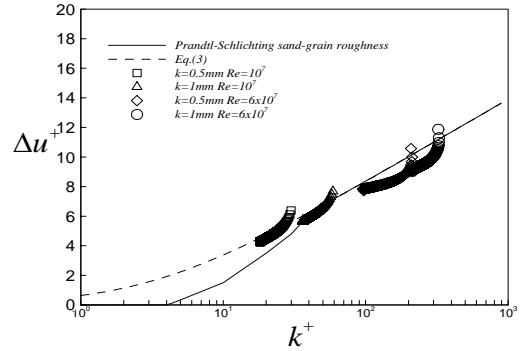
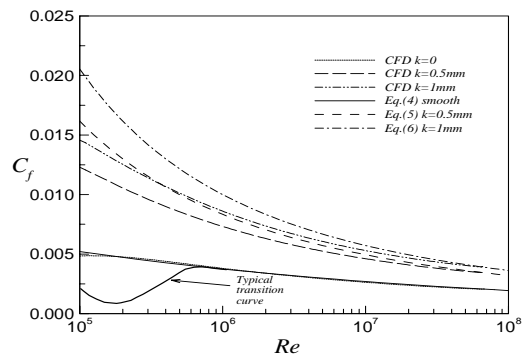Fig. 2 Distributions of Δu^+ corresponding to k^+

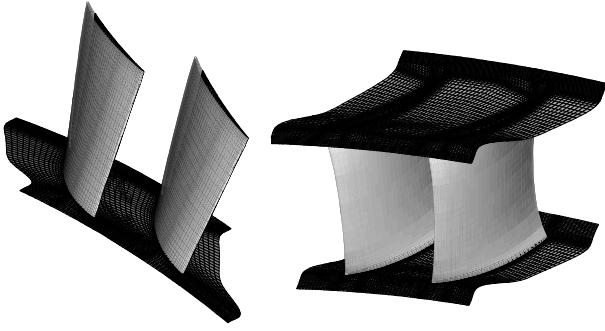Fig. 3 Distributions of C_f corresponding to Re

Fig. 4 Grids of (a) rotor and (b) stator 3rd stage of LSRC
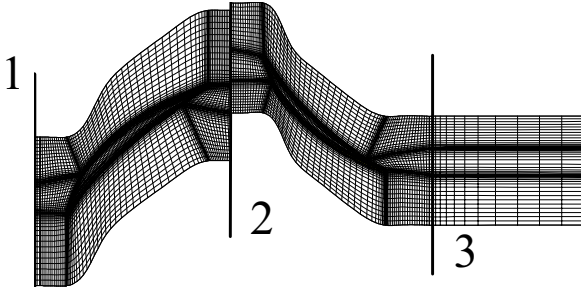

Fig. 5 Blade to blade view of attached grid

especially when roughness height are larger.

Difference between the calculated results and the correlations of Δu^+ and C_f can be explained by performance of the high Reynolds turbulence model and numeric in the calculations. When considering k_s and Reynolds number of $10^6 \sim 10^7$ in general operating conditions of turbo-machine, it can be concluded that roughness model in TascFlow is adequate to expect roughness effects in turbo-machine.

ROUGHNESS EFFECTS ON COMPRESSOR STAGE.

Specification and Configurations for CFD.

The third stage of LSRC (Low Speed Research Compressor) designed by GE is used for the present study. The stator and rotor stages consist of 54 vanes and 74 blades respectively. Shapes of stator vane and rotor blade are three dimensionally designed for high performance. Tip clearances for stator and blade are 1.36% and 0.78% of their spans but in CFD process, tip clearances are not considered. Hub and casing radius are 0.6477 and 0.762m. Fig. 4(a) and 4(b) show CFD grids for stator and rotor with 88x58x36 cells and 96x48x36 cells respectively. In-block is attached at the inlet of rotor and out-block is attached at the outlet of stator for smoother treatment of boundary conditions.

Experimental data at design point is used for boundary conditions; velocity profile from hub to shroud for the inlet and average static pressure for the outlet. The rotating speed is 823 rpm at the design condition. Since this compressor consists of four repeating stages, velocity profile at the outlet should be matched with velocity profile at the inlet. Hence inlet velocity profile is replaced with outlet velocity profile and this process is repeated until inlet velocity profile is reasonably matching with outlet velocity profile. It takes 5 repeating calculations to diminish difference between inlet and outlet velocity profiles within 0.1%. A mixing plane method is used for grid interface between stator and rotor shown in Fig.5. $k - \omega$ high Reynolds turbulence model is used with inlet intensity of 10%.

Results of Smooth Wall

Five different roughness heights are considered for compressor
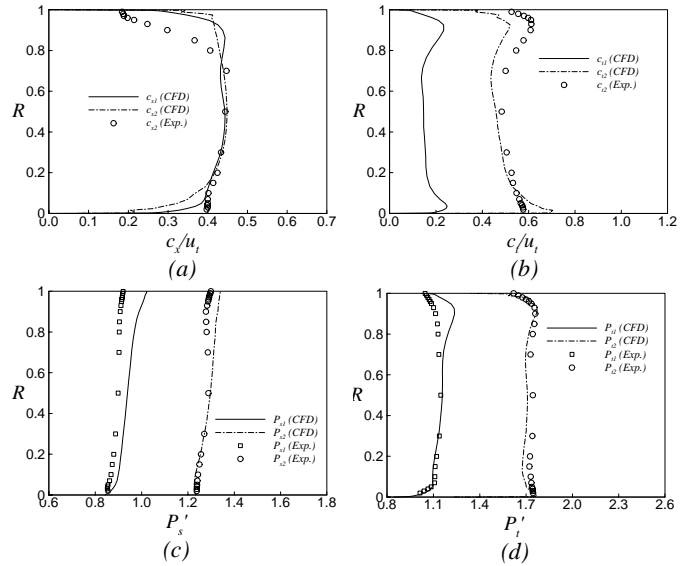

Fig.6-1 Circumferentially averaged value of normalized (a) axial velocity, (b) tangential velocity, (c) static pressure and (d) total pressure at inlet and exit of rotor.
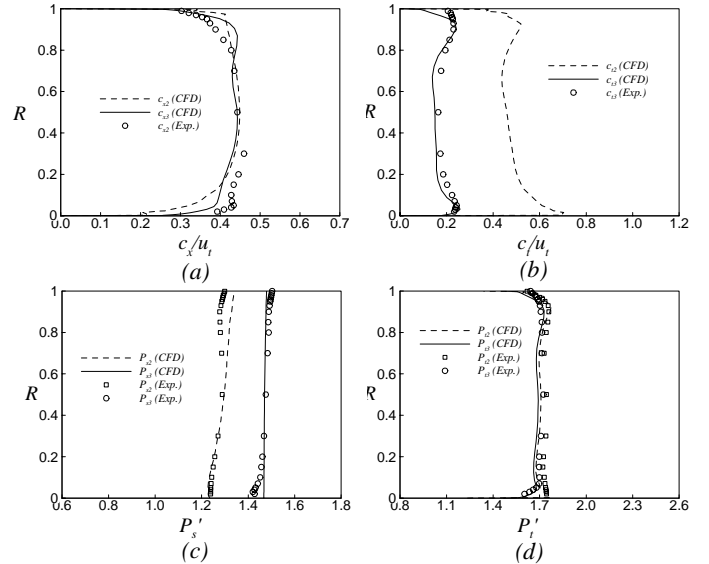

Fig.6-2 Circumferentially averaged value of normalized (a) axial velocity, (b) tangential velocity, (c) static pressure and (d) total pressure at inlet and exit of stator.

stage with smooth wall, k_s =0.1, 0.2, 0.5 and 1.0 mm. To validate CFD results, CFD results of smooth wall are compared with measured data. Distributions of circumferentially averaged velocity profile, static pressure and total pressure are illustrated in Fig. 6-1 and Fig. 6-2 for rotor and stator. Velocity is normalized with blade tip speed, u_t. Also static pressure and total pressure are normalized with dynamic head of reference flow as in Eq. (8).

$$P = \frac{p - p_{ref}}{0.5 \rho_{ref} u_t^2}$$ (8)

where p_{ref} =101326 Pa, ρ_{ref} =1.2 kg/m^3.

Calculated velocity profiles of CFD results are well coincident with the measured data except for tip region of rotor and hub region of stator. Also pressure rise of CFD result is less than that of measured data. It is thought to be due to neglect of tip clearances of rotor tip and stator hub and complicated geometry in the vicinity of hub and tip. Also pitch-wise variation of velocity or pressure is considerably significant that mixing plane approach can cause these differences between CFD results and measured data. It is also expected that if that if the measured profile of pressure distribution
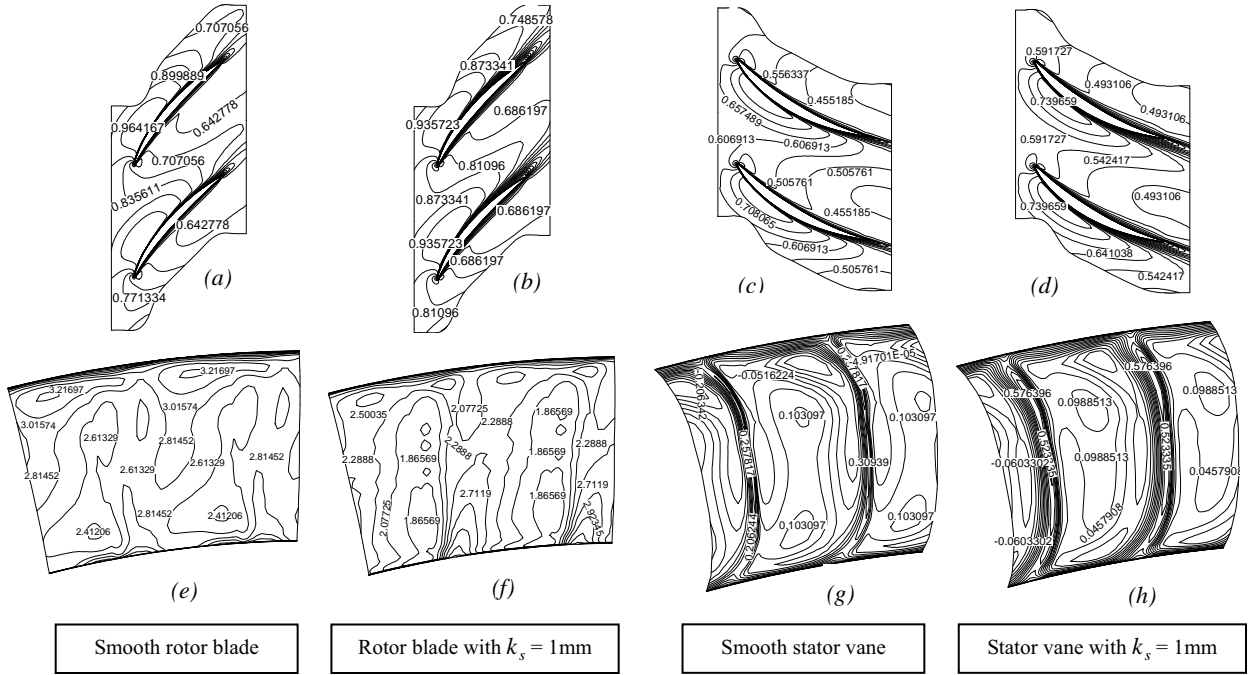
Fig. 7 Distributions of normalized relative velocity at mid-span of (a) smooth rotor, (b) rough rotor, absolute velocity at mid-span of (c) smooth stator, (d) rough stator and normalized total pressure rise at exit of (e) smooth rotor, (f) rough rotor, total pressure loss at exit of (g) smooth stator and (h) rough rotor

at the outlet is used, CFD results can be improved.

Results of Rough Wall

Figs. 7(a), (b), (c) and (d) show contours of normalized velocity at mid-span of rotor and stator for smooth and k_s =1mm cases. Boundary layer thickness is considerably increased due to the blade surface roughness. Thick boundary layer accelerates the core flow and affects deviation angle. Figs. 7(e), (f), (g) and (h) show contours of normalized total pressure rise in the rotor and total pressure loss in the stator defined in Eq. (10).

$$C_{p_{rotor}} = \frac{p_t - p_{t1}}{p_{t2} - p_{s1}}, \ \xi_{stator} = \frac{p_{t2} - p_t}{p_{t2} - p_{s2}} \qquad (10)$$

For smooth case, its contour gradient is not so steep, while rough

blade case shows sharp gradient due to stronger wake. The wake region of high pressure loss forms band-shape in the radial direction. And total pressure rise coefficient of rough case is smaller than that of smooth case that it can be also expected that loss generation would be greater than that of smooth case. Fig. 7 (c), (d), (g) and (h) show normalized velocity at mid-span of stator and

Fig. 9 (a) Distributions of work coefficient

Fig. 9 (b) Distributions of efficiency
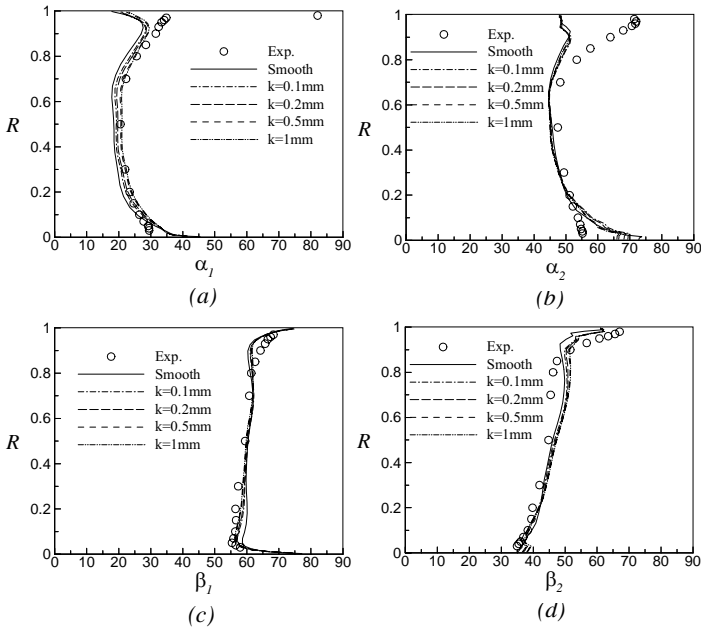

(a)   *(b)*

(c)   *(d)*

Fig. 8 Distributions of circumferentially averaged absolute flow angles at (a) rotor inlet, (b) rotor outlet (c) stator inlet and (d) stator outlet.
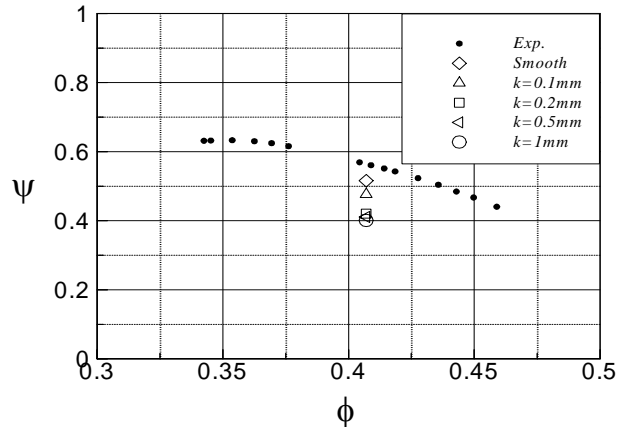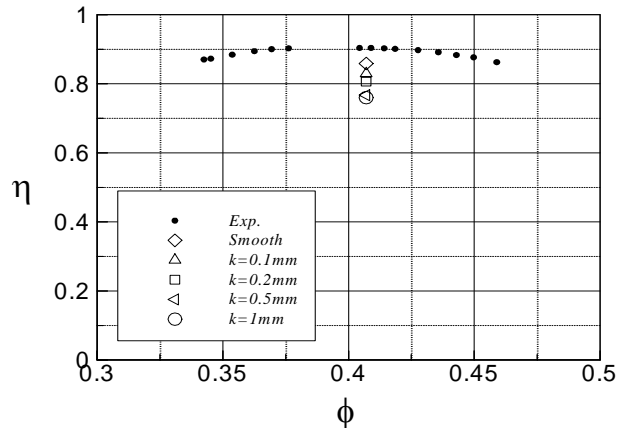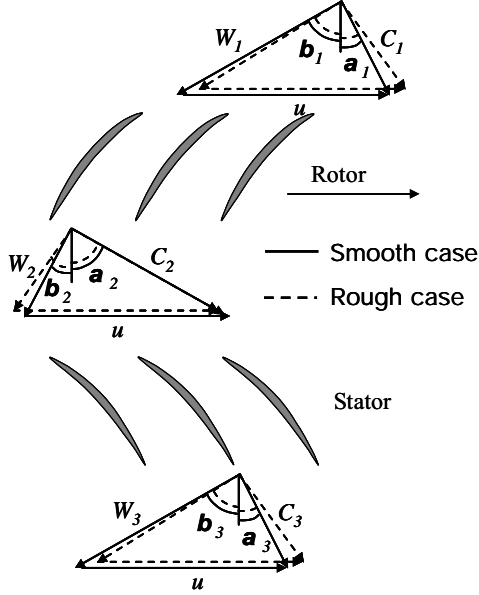
Fig. 10 Velocity triangles of compressor stage

Fig. 11 (a) Contributions of α_1, α_2, ξ on work coefficient drop

Fig. 11 (b) Contributions of α_1, α_2, ξ on efficiency drop

distributions of loss coefficient. Results of the stator are similar to those of the rotor. Wake generation from the rough stator vane is stronger than that from the smooth blade. Loss coefficient for the rough stator case is much greater than that of the smooth blade case, approximately 75% higher. And it is also observed that loss band formed due to wake is much thicker than that of the smooth blade.

Fig. 8 compares circumferentially averaged absolute and relative flow angles at the rotor inlet (stator outlet) and the rotor outlet (stator inlet) for different roughness heights with the measured result. As k_s is increased, β_1 is slightly decreased and β_2 is slightly increased. α_1 is significantly increased compared to other flow angles, whereas α_2 seems to be fixed. Fig. 10 is schematic diagram of velocity triangle of smooth and rough compressor stages. To satisfy calculated results, slight decrease in axial velocity in rough case, should be accompanied.

There still appear considerable deviations over the casing wall. It seems that thick boundary layer of the stator increases the absolute velocity and absolute flow angle at the rotor inlet. But more interesting thing is absolute and relative flow angle at the rotor outlet is not affect by roughness effect so much. It means work transfer to rotor is decreased as roughness height increases by Euler-turbine equation.

To compare overall performance of compressor stage with the measured data, head coefficient and torque efficiency is defined as following.

$$\psi = \Delta h_t / 0.5 u_t^2 \qquad (12)$$

$$\eta = \Delta h_t Q / T\omega \qquad (13)$$

Distributions of Fig. 9(a) show head coefficients corresponding to various roughness heights. When k^+ is in the transitional-roughness regime, in this case k_s =0.1 and 0.2 mm, head coefficient is gradually decreased. But in the meanwhile, k^+ is in the fully rough regime, difference of work coefficient between k_s =0.5mm and 1.0mm is not so significant. Also calculated values of efficiency in Fig. 9(b) show similar trend.

So it can be concluded that even a small amount of roughness in compressor critically affect the performance. Rather when roughness height is sufficiently high enough to be in the fully rough regime, the performance values become less sensitive to roughness. There are also similar reports of sensitivity of the performance to small roughness height. Boynton et. al reported that roughness
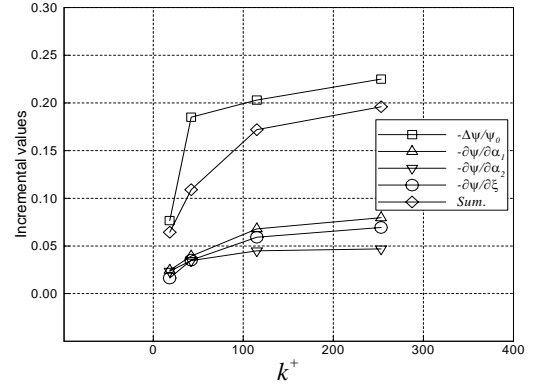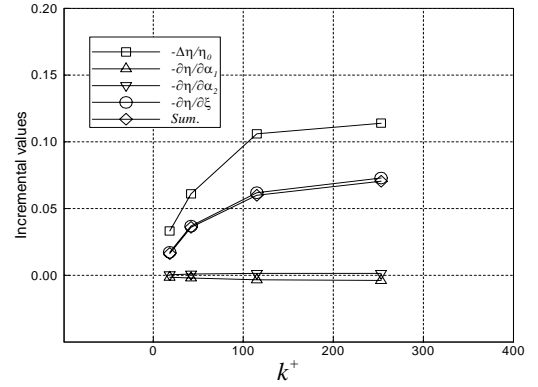
height of 10μm decreases efficiency by 2.5%. And the value of Δu^+ due to roughness is also well agreed with the empirical correlation of Prandtl-Schlichting. Both Boyton's experiment and Prandtl-Schlichting's empirical correlation show rate of change for Δu^+ decreases as k^+ increases. That also implies sensitivity to the performance decreases as roughness height increases.

One Dimensional Analysis

One-dimensional analysis is described in order to quantitatively estimate the effect of the blade roughness on the performance. Total pressure coefficient and efficiency can be presented with a function of absolute flow angles and loss coefficient α_1, α_2, ξ. Assuming that α_1, α_2, ξ are dependent to roughness heights, then total pressure coefficient and efficiency can be arranged as follows.

$$\psi = \Delta p_t / 0.5\rho u_t^2 = \psi(\alpha_1, \alpha_2, \xi) \qquad (14)$$

$$\eta = \frac{\Delta p_t}{\rho u_t c_x (\tan\alpha_2 - \tan\alpha_1)} = \eta(\alpha_1, \alpha_2, \xi) \qquad (15)$$

Total pressure is obtained as follow considering momentum transfer and pressure loss.

$$\Delta p_t = \rho u_t c_x (\tan\alpha_2 - \tan\alpha_1) - 0.5\xi\rho c^2 \qquad (16)$$

Substituting Eq. (16) into Eq. (14) and Eq. (15) leads to Eq. (17) and Eq. (18).

$$\psi = 2\phi(\tan\alpha_2 - \tan\alpha_1) - \xi\phi^2 \qquad (17)$$

$$\eta = 1 - \frac{\phi\xi}{2(\tan\alpha_2 - \tan\alpha_1)} \qquad (18)$$

In order to estimate the effect of the blade roughness on the performance, incremental equations for the head coefficient and

efficiency are needed. By partial differentiating ψ, η with α_1, α_2, ξ, Eq. (20) and (21) are obtained.

$$d\psi = \frac{\partial \psi}{\partial \alpha_1}\bigg)_{\alpha_2, \xi} d\alpha_1 + \frac{\partial \psi}{\partial \alpha_2}\bigg)_{\alpha_1, \xi} d\alpha_2 + \frac{\partial \psi}{\partial \xi}\bigg)_{\alpha_1, \alpha_2} d\xi \quad (19)$$

$$d\eta = \frac{\partial \eta}{\partial \alpha_1}\bigg)_{\alpha_2, \xi} d\alpha_1 + \frac{\partial \eta}{\partial \alpha_2}\bigg)_{\alpha_1, \xi} d\alpha_2 + \frac{\partial \eta}{\partial \xi}\bigg)_{\alpha_1, \alpha_2} d\xi \quad (20)$$

Six partial difference terms in Eq. (19) and Eq (20) can be obtained from Eq. (17) and Eq. (18).

$$\frac{\partial \psi}{\partial \alpha_1}\bigg)_{\alpha_2, \xi} = -2\phi \sec^2 \alpha_1 \quad (21)$$

$$\frac{\partial \psi}{\partial \alpha_2}\bigg)_{\alpha_1, \xi} = 2\phi \sec^2 \alpha_2 \quad (22)$$

$$\frac{\partial \psi}{\partial \xi}\bigg)_{\alpha_1, \alpha_2} = -\phi^2 \quad (23)$$

Other 3 partial differential terms in Eq. (20) can be obtained with similar manner.

Incremental values, $\Delta\alpha_1 = \alpha_{1r} - a_{1s}$, $\Delta\alpha_2 = \alpha_{2r} - a_{2s}$ and $\Delta\xi = \xi_r - \xi_s$ are calculated based on the values of smooth blade case. These incremental values are evaluated at the mid-span to avoid three dimensionality. Also six partial differential terms are calculated with the values of smooth wall.

Fig. 11(a) shows the contribution of each incremental terms of the pressure coefficient with roughness Reynolds number and Fig. 11(b) shows their contributions to the efficiency. Fig. 11(a) shows the most dominant variable affecting the pressure coefficient is the rotor absolute flow angle.

Deviation angle at the stator trialing edge increases due to roughness and exit flow angle as shown in Fig. 12, i.e. inlet flow angle to the rotor increases. Euler-turbine equation shows the work reduction and total pressure coefficient decreases. Reduced outlet absolute flow angle from the rotor blade and increased loss coefficient through the rotor also show important contributions to the pressure coefficient reduction with roughness. Meanwhile, the most dominant variable affecting the efficiency drop is the loss coefficient as shown in Fig. 11(b). The changes in absolute flow angle reduce the denominator, i.e. work transfer, and show indirect effect on the efficiency reduction, however, very small. Also Fig. 11(a) and (b) show there exist other variables sensitive to the performances. Considering Fig. 10, flow coefficient could be one of them.

Since the incremental values are evaluated at the mid-span in the above review, there are need what the most reasonable way to estimate each value is.

We decompose the reduction in pressure coefficients and efficiencies into three components; α_1, α_2, ξ. The inlet and exit flow angles which are determined by flow deviation from the stator and rotor blades. Changes in deviation angle and drag coefficient of cascades due to roughness should be estimated for design and performance prediction of turbo-machines. Further researches are needed.

ROUGHNESS EFFECTS ON TURBINE STAGE.

To investigate roughness effect in turbine stage, similar blades of first stage of industrial gas turbine (501F, Siemens) is considered. The stage consists of 32 nozzle vanes and 72 rotor blades. Hub and casing radius are 0.648m and 0.762 m respectively. Configuration for numerical calculation is almost the same with that of compressor stage. Fig. 12 shows CFD grids which consists of one stator block of 96x66x41, two rotor blocks of 2x112x44x41 and

Fig. 12 CFD grids of 1st stage of commercial gas-turbine

two out-blocks are attached to rotor blocks of 2x26x44x41. Total number of grids is 757,680. Total pressure and total temperature are specified at the inlet boundary and mass flow rate is specified for the outlet boundary condition. k-ω high-Reynolds turbulence model is used with the intensity of 3%. To exclude tip clearance effect on the performance, tip clearance is not considered either. In this turbine case, five different sand-grain roughness heights, smooth wall, 0.01, 0.02, 0.05 and 0.1 mm are considered which cover from transitional-roughness regime to fully rough regime.

Results of smooth wall and rough wall

Fig. 13~Fig. 16 show rotor efficiency and work coefficient, rotor inlet, outlet absolute flow angle, outlet relative flow angle and loss coefficient corresponding to roughness Reynolds number. As shown in Fig. 13, efficiency decreases as roughness height increases, while work coefficient shows opposite trend. This can be easily explained with Euler-Turbine equation.

$$\psi = (h_{01} - h_{02})/0.5u_t^2 = \phi(\tan \alpha_1 - \tan \alpha_2) \quad (24)$$

Kind et al.(1998) reported that roughness height scarcely affects the rotor inlet and outlet relative flow angle of turbine stage. On the other hand, blockage effect due to roughness increases so that relative speed also increases. Fig. 14 shows both of the inlet and outlet absolute flow angle is decreased due to roughness. Fig. 15 shows outlet relative flow angle is scarcely affected. This process can be easily explained with Fig. 17, velocity triangles of smooth and rough turbine stages. As shown in Fig. 17, if it is assumed that β_1, β_2 are not changed a lot and W_1, W_2 are increased due to blockage effect, then both α_1, α_2 can be changed. In this case α_1, α_2 are decreased as shown in Fig. 14. However, decreased quantity of rotor outlet absolute flow angle is much larger than that of inlet, total work transfer is increased from Eq. (24). For this reason, it can be explained why work coefficient increases as roughness height increases. Fig. 16 indicates loss coefficient defined as follows.

$$\xi = (h_{02} - h_{02s})/0.5c_2^2 \quad (25)$$

Aside from increase of work transfer from fluid to rotor, loss generation increases as roughness height increases as expected. And also in turbine case, loss coefficient becomes less sensitive as roughness Reynolds number increases.

One Dimensional Analysis

Similar one-dimensional analysis to see contribution of the inlet absolute flow angle, outlet absolute flow angle and loss coefficient on the rotor stage efficiency defined in Eq. (26). Subscript 1,2 indicates rotor inlet and outlet.
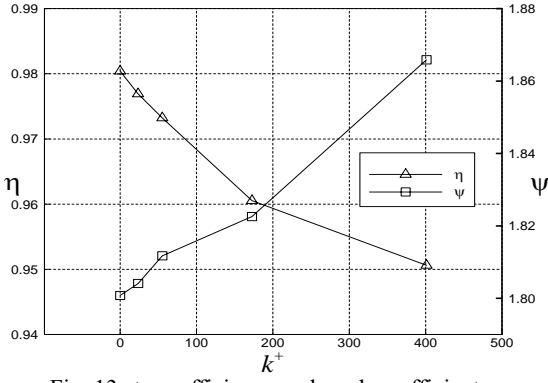
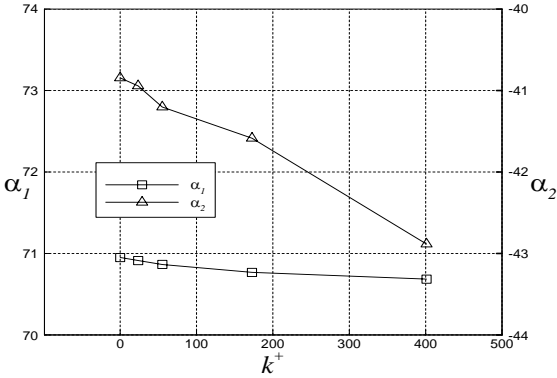Fig. 13 stage efficiency and work coefficient

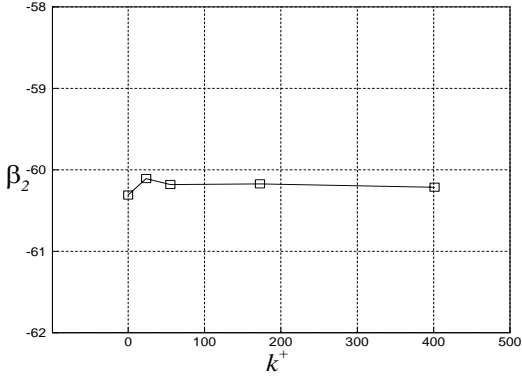Fig. 14 absolute flow angle at inlet and outlet
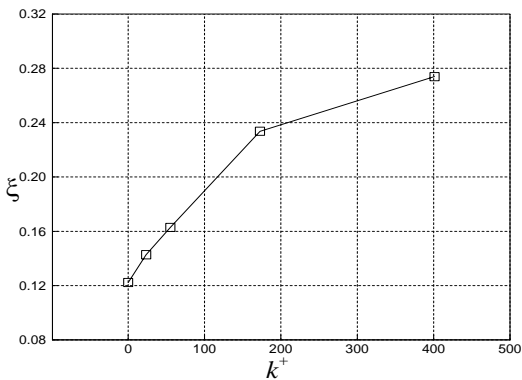

Fig. 15 relative flow angle at outlet of rotor

Fig. 16 Distributions of loss coefficient

$$\eta = \frac{h_{01} - h_{02}}{h_{01} - h_{02s}} = \frac{\phi(\tan \alpha_1 - \tan \alpha_2)}{\phi(\tan \alpha_1 - \tan \alpha_2) + 0.5\xi c_2^2 / u_t^2} \qquad (26)$$

Also like in Eq.(21)~(23) efficiency can be partially differentiated by α_1, α_2, ξ. Eq. (27)~(29), each partially differentiated term indicates their contributions on efficiency

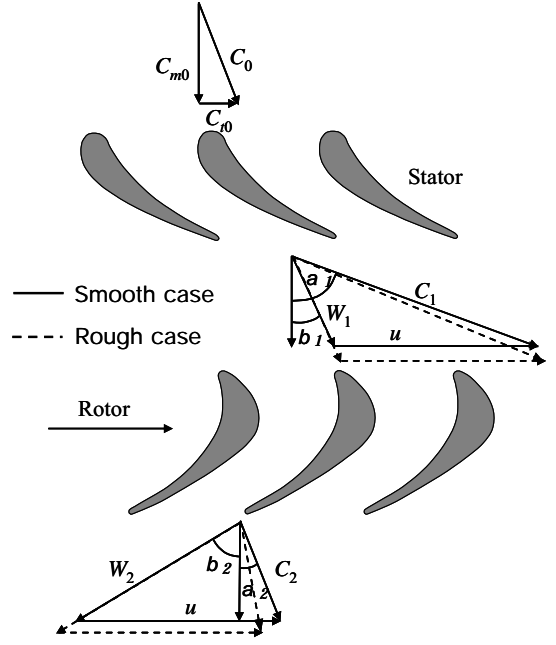

Fig. 17 Velocity triangles of turbine stage

drop of the rotor-stage.

$$\left.\frac{\partial \eta}{\partial \alpha_1}\right)_{\alpha_2, \xi} = \frac{0.5\xi\phi u_t^2 c_2^2 \sec^2 \alpha_1}{\{\phi u_t^2 (\tan \alpha_1 - \tan \alpha_2) + 0.5\xi c_2^2\}} \qquad (27)$$

$$\left.\frac{\partial \eta}{\partial \alpha_2}\right)_{\alpha_1, \xi} = \frac{-0.5\xi\phi u_t^2 c_2^2 \sec^2 \alpha_2}{\{\phi u_t^2 (\tan \alpha_1 - \tan \alpha_2) + 0.5\xi c_2^2\}} \qquad (28)$$

$$\left.\frac{\partial \eta}{\partial \xi}\right)_{\alpha_1, \alpha_2} = \frac{-0.5\xi\phi u_t^2 c_2^2 (\tan \alpha_1 - \tan \alpha_2)}{\{\phi u_t^2 (\tan \alpha_1 - \tan \alpha_2) + 0.5\xi c_2^2\}} \qquad (29)$$
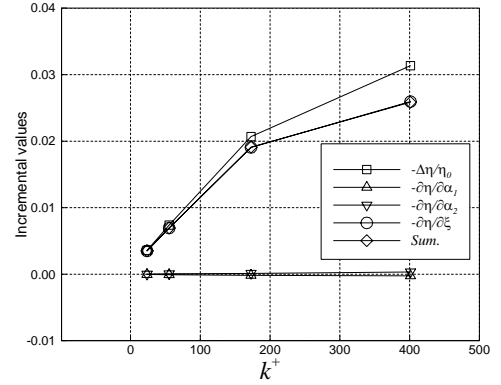

Fig. 18 Contributions of α_1, α_2, ξ on rotor-efficiency drop

Incremental values, $\Delta\alpha_1 = \alpha_{1r} - a_{1s}$, $\Delta\alpha_2 = \alpha_{2r} - a_{2s}$ and $\Delta\xi = \xi_r - \xi_s$ are also estimated at the mid-span based on the values of the smooth blade case. Fig. 18 describes contributions of α_1, α_2, ξ on rotor-stage efficiency. Its result shows very similar trend with that of compressor. Increased work transfer from fluid to rotor scarcely affects the efficiency. Also it shows that additional loss generation dominates efficiency drop and it is very similar trend that of result of the compressor. And difference between sum of incremental terms and stage efficiency is not so large unless k^+ increases. It means that excluding α_1, α_2, ξ, the performance variables of turbine stage are less sensitive to other variables, e.g.

flow coefficient, than compressor when roughness is considered. Further study is needed for other factors that affect the performances of turbo-machines.

CONCLUSIONS

Numerical calculations for compressor and turbine stages are carried out to investigate roughness effect on the performance.

In compressor stage calculations with various roughness heights which cover from the transitional to fully rough regime, even a small amount of roughness affects the head coefficient and efficiency.

One-dimensional analyses are carried out to inspect the contributions of α_1, α_2, ξ. The boundary layer thickness becomes thick with the roughness so that the boundary layer constricts flow passage to change flow angles at the inlet and outlet and generate extra pressure loss. The contributions of change in work transfer and loss generation on the performance, both components are nearly the same amount. But efficiency drop due to roughness is entirely affected by the loss generation..

For the turbine, efficiencies decrease as the roughness height increases, while work coefficients show opposite trend. Efficiency drop due to roughness is also entirely affected by the loss generation

The results are meaningful database to study relationships between the performance variables and wall roughness Reynolds number.

REFERENCES

Bammert, K., and Sandstede, H., 1980, Measurements of the Boundary Layer Development along a Turbine Blade with Rough Surfaces, ASME J. Eng. Power, 102, 978-983.

Schlichting, H., 1979, Boundary Layer Theory, 7th Edition, McGraw-Hill, New York.

Forster, V.T., 1967 Performance Loss of Modern Steam-Turbine Plant Due to Surface Roughness, Proc, Inst. Mech. Engrs. 1966-67, 181, 391-405.

Bammert, K., and Sandstede, H., 1972, Measurements Concerning the Influence of Surface Roughness and Profile Changes on the Performance of Gas Turbine, ASME J. Eng. Power, 94, 207-213.

Kind, R.J., Serjak, P.J., Abbott, M.W.P., 1998, Measurements and Prediction of the Effects of Surface Roughness on Profile Losses and Deviation in a Turbine Cascade, ASME J. Turbomachinery, 120, 20-27.

Nikuradse, J., 1933, Laws For Flows In Rough Pipes, VDI-Forchungsheft 361, Series B, Vol. 4.

Kline, S.J., and McClintock, F.A., Describing Uncertainty in Single Sample Experiments, Mechanical Engineering, January 1953, 3-8.

Denton, J.D., 1993, Loss Mechanisms in Turbomachines, ASME J. Turbomachinery, 115, 621-656

H.J Eum, S.H Kang, 2003, Numerical Study on Tip Clearance Effect on Performance of a Centrifugal Compressor, KSME Journal, vol. 27. pp. 389~397

K.H. Han, 2003 Roughness effect on the performance and flow field of a multistage axial compressor with numerical simulation. M.S Thesis of Seoul National Univ.